Wasit Journal of Engineering Sciences

Journal homepage: https://ejuow.uowasit.edu.iq

COVID-19 detection using machine learning and fusion-based deep learning models

Fatima Raheem Sultan[1], Manaf K. Hussein[2]

Affiliations
[1]Department of Electrical Engineering
College of Engineering
University of Wasit
Wasit, Iraq

Correspondence
[2]Department of Electrical Engineering.
University of Wasit,
Kut, Iraq.

Email:
fatimar302@uowasit.edu.iq

Received
28-February-2023
Revised
13-May-2023
Accepted
11-July-2023

Doi: 10.31185/ejuow.Vol11.Iss2.439

Abstract:

The COVID-19 pandemic has been one of the most challenging crises attacking the world in the last three years. Many systems have been introduced in the field of COVID-19 detection.

In this research, machine learning (ML) and deep learning (DL) models for the detection of COVID-19 with a probability of the presence of COVID-19 are proposed. In the machine learning scenario, the COVID-19 dataset is split into 70% training and 30% testing, and a segmentation process is applied to the CT images in order to get the lung ROI only. The features of CT images are then extracted using Gabor-Wavelet and deep-based features. The SVM classifier is then trained and evaluated. For the deep learning model, the CT images are fed into the model without feature extraction, and three different DL models (CNN, GoogleNet, and ResNet50) are trained and evaluated. Other scenarios are proposed in which the SVM Gabor-Wavelet and deep features are fused, and the three deep learning models are also fused to get better performance. The experiments show that the best model is the deep-based fusion model by which the system achieved 96.4156%, 96.1905%, and 96.1905% for accuracy, precision, and recall, respectively.

Keywords: Machine Learning, Deep Learning, SVM, COVID-19, Model Fusion.

الخلاصة: كانت جائحة COVID-19 واحدة من أكثر الأزمات تحديًا التي هزت العالم في السنوات الثلاث الماضية. تم تقديم العديد من الأنظمة في مجال الكشف عن COVID-19 .

في هذا البحث، تم اقتراح نماذج التعلم الآلي والتعلم العميق للكشف عن COVID-19 مع إعطاء نسب لاحتمال وجود COVID-19. في سيناريو التعلم الآلي، يتم تقسيم مجموعة بيانات COVID-19 إلى 70٪ تدريب و30٪ اختبار، ويتم تطبيق عملية تجزئة على صور التصوير المقطعي المحوسب من أجل الحصول على منطقة الرئة فقط. ثم يتم استخراج ميزات صور التصوير المقطعي المحوسب باستخدام Gabor-Wavelet والميزات العميقة. ثم يتم تدريب مصنف SVM وتقييمه. بالنسبة لنموذج التعلم العميق، يتم إدخال صور التصوير المقطعي المحوسب في النموذج دون استخراج الميزات، ويتم تدريب وتقييم ثلاثة نماذج مختلفة للتعلم العميق هي (CNN, GoogleNet, ResNet). تم اقتراح سيناريوهات أخرى يتم فيها دمج SVM Gabor-Wavelet والميزات العميقة، كما يتم دمج نماذج التعلم العميق الثلاثة أيضًا للحصول على أداء أفضل. أظهرت التجارب أن أفضل نموذج هو نموذج الدمج لأنظمة التعلم العميق الذي حقق النظام بواسطته 96.4156٪ و96.1905٪ و96.1905٪ للدقة والدقة والاسترجاع على التوالي.

1. INTRODUCTION

One of the most important challenges over the past three years was the COVID-19 pandemic. This disease has caused the infection and death of millions of people. The laboratory test polymerase chain reaction (PCR), which is carried out on samples collected from the patient's nose or throat, is now used to identify COVID-19. Results from this PCR test take about a day to be obtained [1]. The high rate of false negatives (those who have COVID-19 but the test says they don't) is one of PCR's numerous drawbacks. PCR tests have a specificity and sensitivity range of 37% to 71%. [2]. On the other hand, because the outcome can be determined a few minutes after the imaging session, computed tomography (CT) and x-ray imaging have become quite fashionable in the diagnosis of COVID-19. In addition, the doctor can see more details about the disease's stage and progression. The COVID-2019 epidemic has put the entire world under a state of containment in an effort to stop further spread and human casualties. Currently, 80% of infections are minor or asymptomatic, 15% require oxygen therapy, and the remaining 5% are serious and necessitate respiratory system support [3]. An illustration of a COVID-19 and standard CT scan is shown in Figure 1.

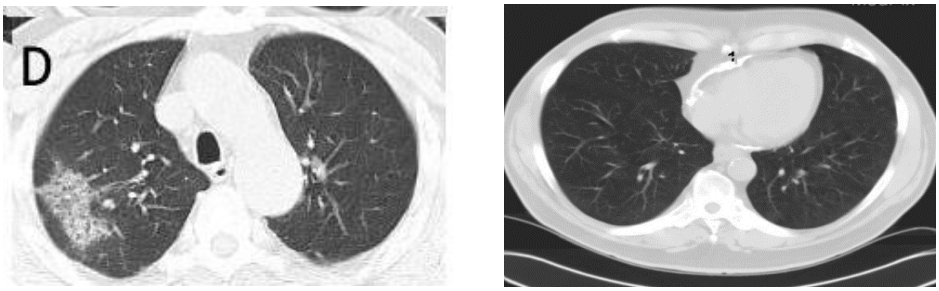

A B

Figure 1: Example of COVID-19 and Normal CT images.

Many researchers have introduced research in the field of COVID-19 detection based on CT or X-ray images. These researchers used Machine learning (ML) and Deep Learning (DL) models to analyses the CT or X-ray images and detect COVID-19.

The deep learning network "Squeeze Net" was used by (Ucar and Korkmaz, 2019) [4] to detect COVID-19 in CT scan lung images. In order to increase detection accuracy, they also used the Bayesian optimization approach inside the network's architecture. The suggested method considered differentiating between pneumonia, non-COVID-19 cases, and COVID-19 cases, resulting in a dataset of 5310 training images and 639 test images. The overall accuracy that was attained was 76.37%. A deep learning-based method for the detection of COVID-19 from X-Ray pictures was proposed by Ozturk et al. in 2020, [5]. They used the DarkNet architecture with changing the convolution layers by adding 17 layers. They also separated each layer's filters. For binary classification issues, the trained model had an accuracy of 98.08%, while for multi-class classification, it had an accuracy of 87.02%. A brand-new deep network dubbed CovidNet that was entirely a convolutional neural network was introduced by Wang et al. in 2020, [6]. They used 13,870 X-ray pictures of patient cases to train their network (Normal and Not-COVID-19). The proposed methodology had a 91.0% sensitivity rate (Recall rate).

A fusion model of the CT lung picture and the textual symptoms was suggested by Mayya and Khozama, 2020, [7]. Only 120 examples from the COVID-19 dataset were used. For the textual model, they employed the Random Forest ML classifier, and for the image model, they used GoogleNet deep learning. A new methodology was used to accomplish the fusion. The results proved the robustness of the proposed system since they got a 4.5% total error rate. Kedia et al., 2021, [8], suggested CoVNet-19 as an ensemble of VGG and DenseNet networks in response to recent advances of more sophisticated designs, particularly ensemble approaches. The moderately large dataset of COVID-19-positive pictures on which CoVNet-19 was trained consisted of 798 CXRs. It's significant to note that the authors compiled their dataset from numerous, occasionally overlapping public sources. Several COVID x-rays have been copied as a result. Their best efforts yielded an F1-Score of 0.9891 for three-class categorization.

Transfer learning of CheXNet was introduced by Haghanifar et al., 2022, [9]. a dataset with 1326 cases was used to investigate the X-Ray pictures. The U-Net architecture is used to extract features from the X-Ray images for the main model after the images have been pre-processed using the CLAHE algorithm. Using the concept of transfer learning, another CheXNet model was also trained. The findings indicated that the F1-score detection rates for COVID-19 and pneumonia illnesses, respectively, had gained accuracy of 86.21% and 96.56%. A deep-learning-based algorithm for

COVID-19 identification was proposed by Bhattacharyya et al. in 2022 [10] utilizing a collection of X-Ray images gathered from several online data sources. In the first step, the X-Ray images were segmented using the conditional generative adversarial network (C-GAN). In the second step, a pipeline consisting of VGG-19 and a key-point feature extractor was built and trained using the segmented images. The VGG-19 model's accuracy after training was 96.6%.

The remaining sections of this paper are structured as follows: Section 2 describes the key characteristics of COVID-19 found in CT lung images; Section 3 describes the machine learning COVID-19 detection step; Section 4 describes the deep learning COVID-19 detection step; Section 5 presents the proposed system's implementation and results; and Section 6 lists the conclusions.

2. COVID-19 CT IMAGE MAIN FEATURES

Physicians used many image features inside the CT lung image to detect COVID-19. These features are the Ground Glass (GG), consolidations, Reticular pattern, an Air bronchogram, a Crazy paving pattern, Pleural changes, Airway changes, an Air bubble sign, and Lung Nodules. Ground glass (GGO) is one of the most common marks inside CT images that correspond to COVID-19 infection. The term "GGO" refers to hazy patches in the lungs that have a little increase in density but do not obscure the bronchial and vascular boundaries [10]. The case in which the alveolar air is replaced with pathological fluids, cells, or tissues is known as consolidation [10]. It is characterized by an increase in pulmonary parenchymal density that hides the borders of the underlying arteries and airway walls. With an incidence rate of 2–64% [11], multifocal or segmental consolidation dispersed in subpleural locations or along broncho-vascular bundles is typically observed in COVID-19 patients. Reticular pattern, which appears as a collection of numerous tiny linear opacities on CT scans, was characterized as enlarged pulmonary interstitial structures such as interlobular septa and intralobular lines. This pattern's development may be related to interstitial lymphocyte infiltration, which thickens the interlobular septum [12].

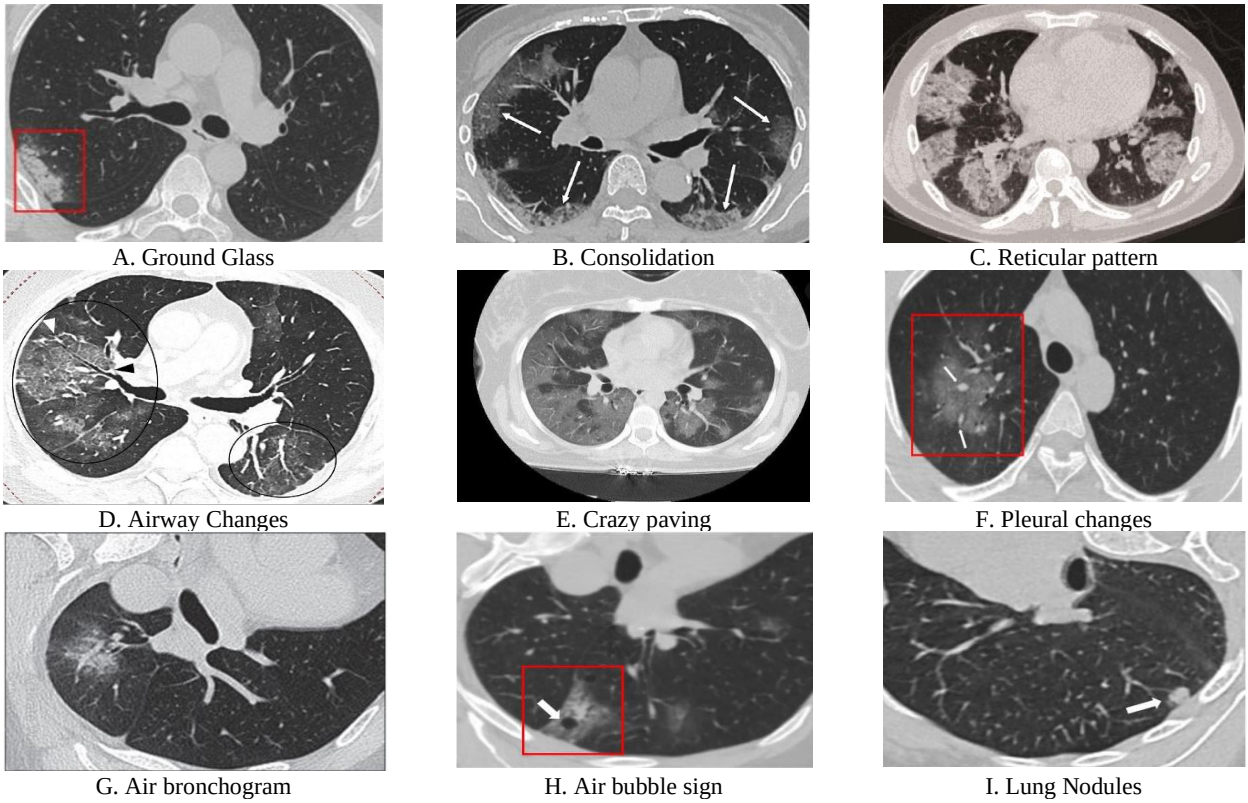

Figure 2: Examples of some CT features in COVID-19 patients [10], [12], [17-19].

The most frequent chest CT symptom of COVID-19, second only to GGO and consolidation, is the reticular pattern with interlobular septal thickening, according to a number of publications [13]. Another CT manifestation of COVID-19 was described as an air bronchogram, which is a pattern of air-filled bronchi on a background of hazy airless lung tissues [10]. An imaging result that points to the progression of COVID-19 are the "crazy-paving pattern," which consists

of thicker interlobular septa and intralobular lines overlaid on diffuse ground-glass attenuation. In their studies, recent examinations found that 5–36% of COVID-19 patients had crazy paving patterns [14]. Crazy paving patterns can also herald entry into the progressive or peak stage of COVID-19 when combined with diffuse GGO and consolidation. Pleural thickness and pleural effusion are among the pleural alterations observed in COVID-19, with the former symptom being more common. A recent study that included 81 COVID-19 patients found that 32% of them showed pleural thickening and 5% showed pleural effusion [15].

Bronchiectasis and thickening of the bronchial wall are the two types the airways. Some COVID-19 instances have been associated with bronchiectasis, whereas 10% to 20% of COVID-19 patients have been associated with bronchial wall thickening. The pathogenesis of tractive bronchiectasis can be caused by inflammatory damage to the bronchial wall and bronchial obstruction, which leads to the loss of the bronchial wall's structure, the growth of fibrous tissue, and fibrosis [16]. A small air-containing gap in the lung known as the "air bubble sign" may be caused by the pathological enlargement of a physiological space, a cross-section of the bronchiectasis, or it may be connected to the consolidation-resorption process. Lung nodules are rounded or irregular opacity with non-uniform edges with small measurements (3 cm). These nodules are commonly associated with pneumonia. Figure 2 shows examples of those previous features of lung CT images of COVID-19 patients [10], [12], [17-19].

3. IMAGE CAPTURING

Medical COVID-19 imaging like CT and X-ray is used for the diagnosis of COVID-19. The main problem is that there are millions of CT images and the physicians can't handle this large amount of data to judge the new CT cases. For this reason, ML algorithms are used to help them make decisions in the diagnosis of COVID-19. Different ML methods were used by researchers for the aim of COVID-19 detection. The main rule of these systems was to distinguish between COVID-19 and non-COVID-19 cases or at least differentiate COVID-19 from normal cases.

There are many steps in any ML COVID-19 detection system [20]:

1. Pre-processing: in this step, the CT image is manipulated to get a better version of it. Some filtering and morphological operations are done to enhance those images.
2. Segmentation: in this step, the ROI which represents only the lung tissue is extracted and the rest of the CT image is dropped.
3. Feature extraction: After getting the ROI of the lung tissue, the image features are extracted using some effective algorithms like Wavelet, Gabor, Scale-invariant features, etc.
4. Training and classification: The extracted features are loaded into a selected classifier which is trained to distinguish the normal tissues from the COVID-19 ones. The better classifier to use, the better performance we get.
5. Testing: in this step, the trained classifier is tested using new cases of non-COVID-19 and COVID-19. The evaluation process should also be performed in order to assist the final system.

Commonly, there are two types of training and learning in ML, supervised and unsupervised learning. In the first type, the input and output (CT images and their classes) should be passed to the classifier, while in the second one, the only input that is passed to the classifier is the CT images. The ML classifier should classify them into classes depending on some similarity metrics.

3.1. MACHINE LEARNING MODEL- SUPPORT VECTOR MACHINE (SVM)

The first machine learning model is the SVM classifier. Support-vector machines (SVMs, also known as support-vector networks [20]) in machine learning are supervised learning methods with corresponding learning algorithms that evaluate data for regression and classification. SVM was first developed by Vladimir Vapnik and colleagues at AT&T Bell Laboratories. An SVM training algorithm creates a model that categorizes new samples into one of two categories based on a collection of training examples constituting a binary linear classifier. SVM assigns training samples to spatial coordinates in order to maximize the distance between the two classes. Then, based on which side of the split they fall, new samples are projected into that same area and estimated to belong to a category. The SVM can perform non-linear classification problems besides binary classification, and this is due to the modification that was applied to the algorithm by entering what is called the "kernel function".

In SVM, the margin is an essential part. It refers to the distance between two classes and can be defined by the support vectors. Support vectors are samples of the two classes that are the most similar to each other. Figure 3 shows the margin and support vectors between two classes of a classification problem.

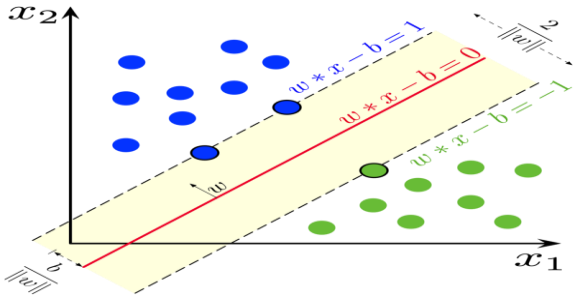

Figure 3: The margin and the Support Vectors.

Figure 3 shows the margin between the positive and negative classes. It can be computed as 2/ ||W|| where W is the normal vector to the hyperplane. The positive and negative hyperplanes of the problem in Figure 3 can be formulated as Eq.1 and Eq.2 show.

$$W * x - b = 1 \quad (1)$$

$$W * x - b = -1 \quad (2)$$

Any sample that is located over the hyperplane of Eq.1 is considered to be of the positive class, while any sample that is located below the hyperplane of Eq.2 is considered to be of the negative class. Samples that are located directly on one of these two hyperplanes are called the support vectors. The greater distance between the support vectors of the two classes, the bigger the margin. So, if the margin is large, the classification will be easier and the samples will be classified in the very ideal way. In practice, the margin can be small and the support vectors can be very close. In our study, we will use the SVM to classify the two different classes (COVID-19 and Not-COVID-19). So, we will use the linear SVM

4. DEEP LEARNING FOR COVID-19 DIAGNOSIS

Many deep learning networks were used for the aim of COVID-19 prediction and diagnosis. The textual dataset for COVID-19 prediction includes symptoms. The dataset includes images for use in detection and diagnosis. Since the feature extraction stage is carried out inside the DL model using the convolution layers, the deep learning COVID-19 system differs in several steps from the machine learning (ML) systems.

4.1. DEEP LEARNING CNN CONCEPT

The main DL network is CNN. All next networks are derived from CNN. The main architecture of CNN consists of the following parts:

1. Input layer: in our system, the input is the lung CT image.
2. Convolution layer: in which many filters with specific kernel sizes are applied to the input CT image to get the feature-extracted CT image. The output of this layer is called the activation maps or activation records.
3. The pooling layer: in which the convolution result is minimized and down-sampled into smaller sizes depending on the pooling factor. Two different methods of pooling have existed (max pooling and average pooling). More explanation will be listed in the next chapter.
4. The non-linear activation function: the activation function is applied to the pooled activation maps in order to remove undesired pixels.
5. Fully-connected layer: This layer is placed after many convolution-pooling combinations in order to transform the final activation record into one feature vector.
6. Classification layer: in this layer, the "softmax" activation function will be used to give each class of the targets a ratio expressing the matching score between 0 and 1. As a result, the final prediction is based on the class with the highest score (COVID-19 or non-COVID-19).
   An activation function must be present in each layer of the CNN in order to transfer the output of each convolutional layer and eliminate the undesirable values. The non-linear "Relu" function, whose well-known activation function follows each convolution layer, has a straightforward calculation (max (value, 0)), meaning that any convolution result that is less than 0 will be converted to 0. The probabilities of each

output must be calculated at the conclusion of each CNN network, and the class with the highest probability must be chosen as the final prediction. This is done using a "softmax" activation function. Figure. 4 displays the architecture of a convolutional neural network (this architecture is general and is not the only one) [21].

the architecture of a convolutional neural network (this architecture is general and is not the only one) [21].

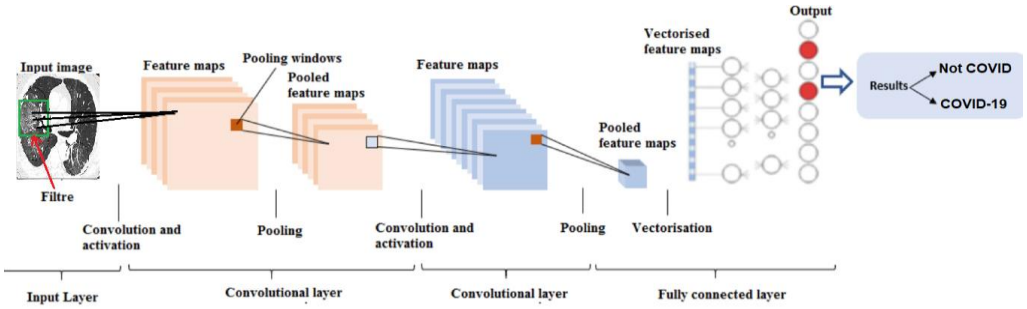

Figure 4: General architecture of convolutional neural networks [21].

Numerous image recognition applications have made use of various CNN network types. We advise utilizing three various forms of them in our investigation (the original CNN, GoogleNet, and ResNet50 architectures).

GoogleNet is a kind of convolutional neural network with 22 layers, and it was first developed by Szegedy et al. [22]. GoogleNet has five convolutional layers. This network's input is 224*224 in size. The primary idea behind this network is the inception layer. The computations are carried out concurrently in the inception layer. The size of the image is reduced to 112*112 by the first convolution layer of the GoogleNet, which consists of 64 filters of size 7*7. The pooling layer follows, which shrinks the input size to 56*56. The second convolution has an input size of 56*56*192 and 192 filters. The image size is decreased to 28*28*192 by the maximum pooling layer. A 256 filter is present in the initial conception layer, yet the image is only 28*28*256 in size. Up until the last inception layer, which is 7*7*1024, the subsequent inception layers maintain the same architecture. The average pooling layer, which serves as the fully linked layer, is the following layer; its output has a size of 1*1*1024. The output size is increased to 1000 samples by using the dropout layer to remove 24 neurons. The classification layer, the last layer, uses the "Softmax" function to assign the input image to the appropriate class [22].

ResNet50 is a type of residual unit that was first invented by Hu et al. [23]. ResNet50 consists of 50 layers, including 48 convolution layers, one max pooling layer, and one fully-connected layer. The central principle of ResNet50 is the use of residual units, which solves the vanishing gradients issue that plagued earlier deep networks. In a gradient-vanishing problem, the gradient gets less as you add more layers; eventually, it disappears, and the training stops updating weights. Three convolutional layers are skipped as the input is forwarded using a connection, and the value of this connection is added to the output of these layers to avoid the gradient from vanishing. The identification connection of the ResNet50 is shown in Figure 5.

layer name	output size	50-layer	101-layer
conv1	112×112	7×7, 64, stride 2	
conv2_x	56×56	3×3 max pool, stride 2	
		$\begin{bmatrix} 1\times1, 64 \\ 3\times3, 64 \\ 1\times1, 256 \end{bmatrix}\times3$	$\begin{bmatrix} 1\times1, 64 \\ 3\times3, 64 \\ 1\times1, 256 \end{bmatrix}\times3$
conv3_x	28×28	$\begin{bmatrix} 1\times1, 128 \\ 3\times3, 128 \\ 1\times1, 512 \end{bmatrix}\times4$	$\begin{bmatrix} 1\times1, 128 \\ 3\times3, 128 \\ 1\times1, 512 \end{bmatrix}\times4$
conv4_x	14×14	$\begin{bmatrix} 1\times1, 256 \\ 3\times3, 256 \\ 1\times1, 1024 \end{bmatrix}\times6$	$\begin{bmatrix} 1\times1, 256 \\ 3\times3, 256 \\ 1\times1, 1024 \end{bmatrix}\times23$
conv5_x	7×7	$\begin{bmatrix} 1\times1, 512 \\ 3\times3, 512 \\ 1\times1, 2048 \end{bmatrix}\times3$	$\begin{bmatrix} 1\times1, 512 \\ 3\times3, 512 \\ 1\times1, 2048 \end{bmatrix}\times3$
	1×1	average pool, 1000-d fc, softmax	
FLOPs		3.8×10^9	7.6×10^9

Figure 5: ResNet50 residual unit architecture [23].

4.2. MODEL EVALUATION

To evaluate the trained models, the following evaluation metrics are used:

- TP: true positives are the number of correctly accepted COVID-19 samples among all COVID-19 test samples.
- TN: true negatives are the number of correctly rejected Not-COVID-19 samples among all Not-COVID-19 test samples.
- FP: false positives are the number of incorrectly accepted test samples that are actually Not-COVID-19.
- FN: false negatives are the number of incorrectly rejected test samples that are in real COVID-19 samples.

Accuracy: Accuracy is the general concept of the performance and is given in Eq.3. Precision: Precision is the number of TP to the total number of TP and FP; it's given as Eq.4 illustrates. Recall: is the number of TP to the total number of TP and FN, it's given as Eq.5 illustrates.

$$Accuracy = \frac{TP + TN}{TP + TN + FP + FN} \tag{3}$$

$$Precision = \frac{TP}{TP + FP} \tag{4}$$

$$Recall = \frac{TP}{TP + FN} \tag{5}$$

5. RESULTS AND DISCUSSION

Figure 6 illustrates the proposed COVID-19 detection system architecture. The SVM ML model and the CNN-based DL architecture will be trained using the segmented images of the COVID-CT image dataset. The dataset will be split into training and test datasets. The training dataset will be used to train models, while the test dataset will be used to evaluate them. For the SVM classifier, the image features are extracted using two different feature extraction methodologies. In the first one, the Gabor-Wavelet features are extracted, while in the second one, the deep features are proposed. For the CNN-deep model, the feature extraction is performed inside the deep network and there is no need to perform any feature extraction step.

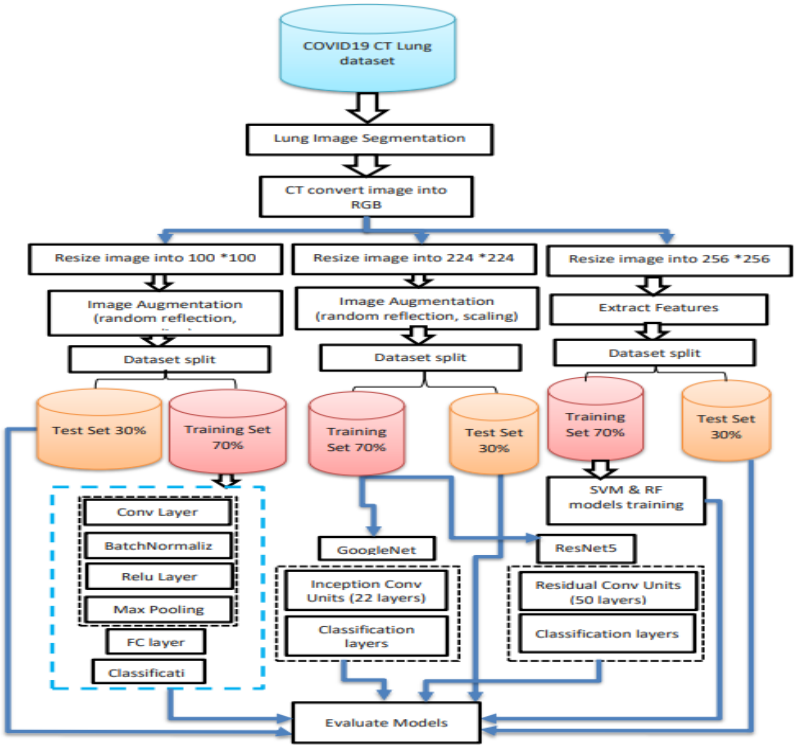

Figure 6: The proposed system architecture.

5.1. CT LUNG IMAGE DATASET

Due to the fact that there are many COVID-19 image datasets, the choice is not easy. To choose a suitable dataset, we define many conditions to acquire the dataset.

1. The dataset must contain not only COVID-19 and Normal images, but also other Not-COVID diseases (influenza, lung inflammation, pneumonia, etc.). This condition makes the challenge harder and the classification problem will be more complicated (this is suitable for actual medical cases).
2. Images of the dataset should be collected from different sources and different acquisition devices.
3. Image format could be of any format and any size.

The previous conditions guide the search for the best dataset. The "COVID-CT" dataset, which is accessible at [24], is the ultimate option. The dataset contains 216 different medical cases represented by 349 COVID-19 and 392 Not-COVID-19 images. The Not-COVID-19 cases could be healthy or suffer from other lung conditions. This dataset, which was collected from several CT imaging machines and from different nations, is completely free. The images come in two formats and don't have a set size (.jpg and .png).

5.2. CT IMAGE SEGMENTATION

In the lung segmentation step, many pre-processing and segmentation processes are applied in order to get the final lung region. In the first step, the image is read and filtered using the median filter (5*5) in order to smooth the little gray changes in the lung image. The smoothed image is then thresholder using a dynamic threshold. The dynamic threshold is obtained using the function "graythresh". After that, the border of the image is cleared of any extra pixels that don't belong to the lung region. This operation is done using the "imclearborder" function. The next operation is image filling, in which the black holes inside the white regions are filled and the lung regions are obtained without any holes. This step is done using the "infill" morphological operation. The final mask obtained in the previous step is applied to the original image in order to get the final lung ROI. Figure 7 shows the result of segmenting a CT lung image with all the previous steps.

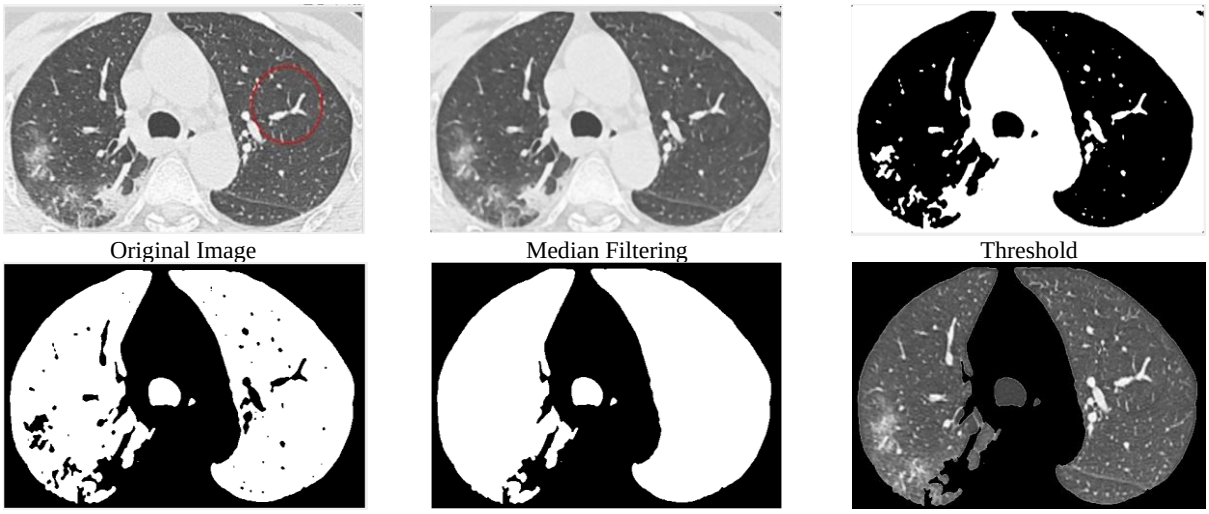

Figure 7: Result of segmenting a lung CT image of the COVID-19 dataset.

5.3. FEATURE EXTRACTION STEP

In the feature extraction step, two different features will be extracted from the segmented CT images. The Gabor-Wavelet features and the deep features. Figure 8 illustrates the steps of feature extraction. Before training the classifier, the features of the CT lung images must be extracted using the Gabor and Wavelet features. The size of the extracted feature vector is 518*88 for training images and 223*88 for test images. Each feature vector has 88 features.

Figure 9-A illustrates an example of the feature vector of two CT images of COVID-19 corresponding to the same medical case. The feature vector of COVID-19 takes a similar shape. On the other hand, in Figure 9-B there is an example of two Not-COVID-19 feature vectors (which are somehow different from COVID-19 features and similar to

each other's). The main problem with these features is that they are similar in some parts of the feature vector. This will cause some degradation to the performance of the classification step.

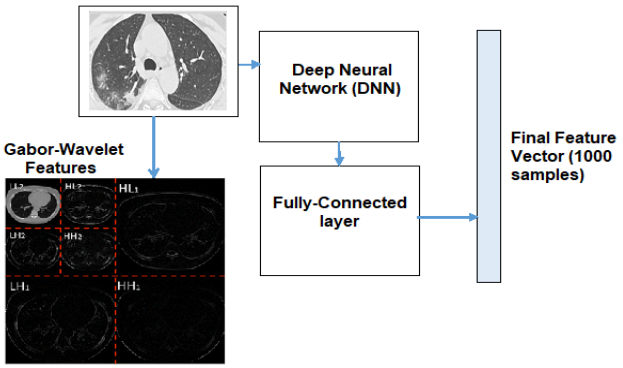

Figure 8: Two different types of features of a Lung CT sample of the dataset.

The second type of feature is the deep features, which are extracted using deep networks. The GoogleNet deep learning model is used to extract deep features from CT lung images. The GoogleNet has many layers, but the " loss3-classifier" is the desired layer from which we can extract the final feature vector. Figures 9-C and 9-D. Figure 9 proves the fact that the deep features have much more information compared to Gabor-Wavelet features. Now the Wavelet and deep features are ready for the next step (training scenarios).

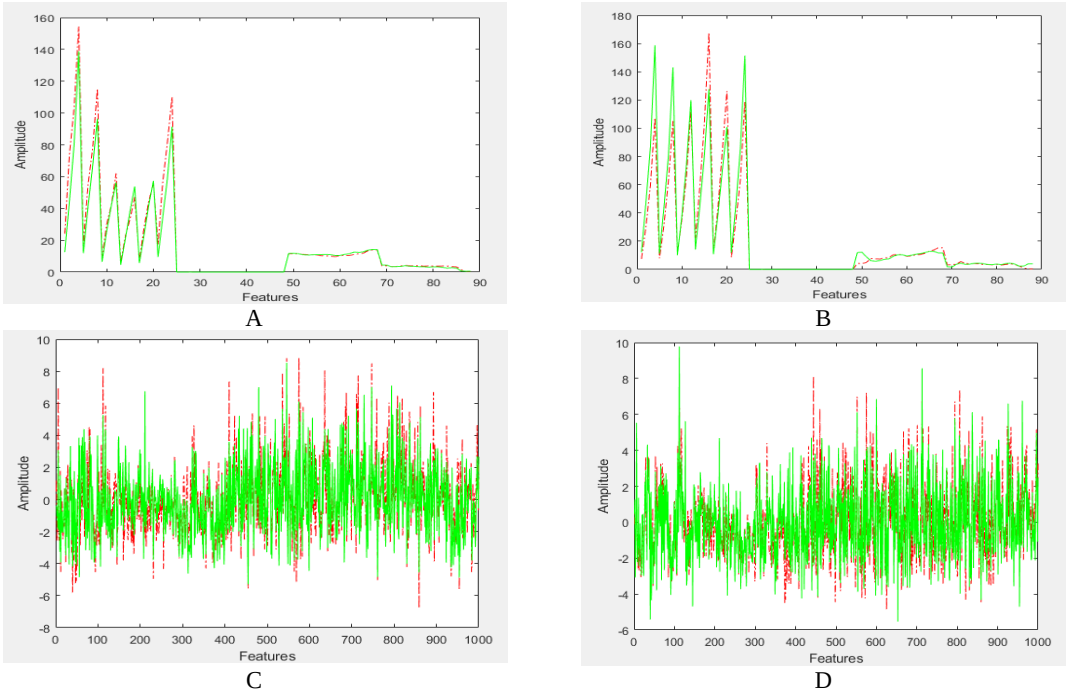

Figure 9: Feature vectors of A. Gabor-Wavelet features of COVID-19 samples, B. Gabor-Wavelet features of Not-COVID-19 samples, C. Deep features of COVID-19 samples, D. Deep features of Not-COVID-19 samples.

5.4. TRAINING SCENARIOS

In our study, we suggest using three different classifiers (SVM and Deep networks). The following training scenarios are suggested.

1. Training the SVM model using original lung images with Gabor-wavelet features.
2. Training the SVM model using original lung images with deep features.
3. Training many deep networks using original lung images.
4. Fusion of 1 and 2.

5. Fusion of all deep learning models.
6. Training models using the segmented Lung CT images.

In all scenarios, the dataset is split into 70% for training and 30% for testing.

5.4.1. SVM SCENARIOS

The SVM classifier was originally created to classify only two classes (binary classification). In our problem, the number of classes is two (COVID-19 and Not-COVID-19). The SVM model is trained using the following parameters:

- 'Kernel Function': 'polynomial', which means that our classification problem kernel function will be polynomial.
- 'Polynomial Order': 4 which is the number of classes + 2. The polynomial order refers to the complexity of the relation between the target (output) and the predictors. We choose the highest number (4) since our classification problem is complicated. After trying 2,3 and 4 as order, we find that 4 is the most suitable polynomial order.
- 'Kernel Scale': 'auto', which means that the algorithm will automatically choose a scale number to divide the training sample by it in order to do the scaling step.
- 'Standardize': true, by setting this parameter as true the algorithm will scale the predictors by the weighted mean and standard deviation of the column.
- 'Score Transform': 'logit', so that we can compute the score of the predicted sample as a value between 0 and 1 (0% to 100%). Table 1 includes the results of testing the SVM model trained using the Gabor-Wavelet features.

Table 1: Evaluation of trained SVM model using the Gabor-Wavelet and deep features.

Model	TP	TN	FP	FN	Precision %	Recall %	Accuracy %
SVM Original GW-Features	83	98	20	22	80.5825	79.0476	81.1659
SVM Original Deep-Features	89	103	15	16	85.5769	84.7619	86.0987
Fusion	92	110	8	13	92	87.6190	90.5830

GW: Gabor-Wavelet.

The results indicate that the precision, recall, and accuracy are low. The trained SVM model using Gabor-Wavelet features has some performance degradation. Table 1 shows that the fusion of the Gabor-Wavelet features with the deep learning features increases the accuracy by 4.48%.

5.4.2. COMPARE THE ORIGINAL LUNG CT-TRAINED MODEL WITH THE SEGMENTED CT-TRAINED MODELS

In order to show the difference between using the segmented lung CT images and the original ones, we repeated the SVM scenarios. Table 2 shows a comparison between the SVM models based on the original dataset and the SVM-trained models based on the segmented lung images. Table 2 shows that using the segmented lung CT images decreases the performance of all models. The best conclusion here is that using the original lung CT images is better than using the segmented ones.

Table 2: A comparison between the SVM models based on the original dataset and the SVM-trained models based on the segmented lung images.

Model	TP	TN	FP	FN	Precision %	Recall %	Accuracy %
SVM (Gabor-Wavelet) original images	83	98	20	22	80.5825	79.0476	81.1659
SVM (Gabor-Wavelet) segmented images	61	71	37	42	62.2449	59.2233	62.5592
SVM (deep features) original images	89	103	15	16	85.5769	84.7619	86.0987
SVM (deep features) segmented images	66	80	28	37	70.2128	64.0777	69.1943

5.4.3. TRAINING MANY DEEP NETWORKS USING ORIGINAL LUNG IMAGES

In this scenario, three different deep networks are used (Convolutional Neural Networks (CNN), GoogleNet and ResNet50). Table 3 includes the results of evaluating the proposed deep learning models.

Table 3: Evaluation of trained deep learning models.

Model	TP	TN	FP	FN	Precision %	Recall %	Accuracy %
CNN	89	111	7	16	92.7083	84.7619	89.6861
GoogleNet	96	105	13	9	88.0734	91.4286	90.1345
ResNet50	94	108	10	11	90.3846	89.5238	90.5830
Fusion	101	114	4	4	96.1905	96.1905	96.4126

Table 3 proves the fact that the ResNet50 model has the best performance compared to GoogleNet and CNN. Moreover, all CNN models have better performance than the SVM ML model. Besides that, the fusion of all deep networks increases the accuracy by 5.82% compared to the best DL model (ResNet50). The proposed methodology presents the detection results as a probability (percentage of COVID-19 presence). Figure 10 includes some examples of the output of the SVM model and the best model (the deep fusion model), with a probability of COVID-19 percentage in each sample. Figure 10 shows that the DL model is better not only in the detection accuracy but also in the probability of COVID-19 presence in the test image.

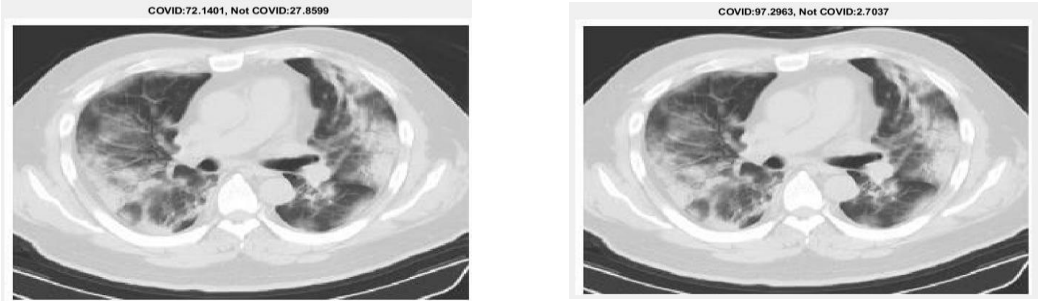

A. SVM model B. Deep fusion model

Figure 10: Example of the detection result of the ML and DL model with corresponding COVID-19 probabilities.

6. CONCLUSION

In this paper, a new COVID-19 detection system is presented. The study suggests using both machine learning and deep learning models and making a performance comparison between them. The proposed methodology consists of many steps. In the first step, the COVID-19 dataset is collected taking into account the COVID-19 cases and other Not-COVID-19 cases (not only the normal situations). In the second step, the lung CT images are segmented using morphological-based processing operations. For the ML model, a feature extraction step is required. The study proposes using a combination of Gabor-Wavelet features and deep-based features. In the training step, the dataset is split into training and testing, and different training scenarios are proposed using the SVM, CNN, GoogleNet, and ResNet50 models. The results indicate that the best model is the deep-based fusion model with 96.4126% accuracy. In this study has one limitation since the deep models are used without any modification in their architecture.

7. RECOMMENDATIONS

To improve the accuracy of the proposed methodology, we suggest modifying the deep-based models by changing learning parameters, layers and even some activation functions. Future research may concentrate on the detection of additional illnesses like pneumonia and lung inflammation.

8. References

[1] Benmalek, E., Elmhamdi, J., & Jilbab, A. (2021). Comparing CT scan and chest X-ray imaging for COVID-19 diagnosis. *Biomedical Engineering Advances*, 1, 100003.

[2] Li, Y., Yao, L., Li, J., Chen, L., Song, Y., Cai, Z., & Yang, C. (2020). Stability issues of RT-PCR testing of SARS-CoV-2 for hospitalized patients clinically diagnosed with COVID-19. *Journal of medical virology*, 92(7):903-908.

[3] Grewal, M., Srivastava, M. M., Kumar, P., & Varadarajan, S. (2018). Radnet: Radiologist-level accuracy using deep learning for hemorrhage detection in ct scans. *In 2018 IEEE 15th International Symposium on Biomedical Imaging (ISBI 2018)*, 281-284.

[4] Ucar, F., & Korkmaz, D. (2020). COVIDiagnosis-Net: Deep Bayes-SqueezeNet-based diagnosis of the coronavirus disease 2019 (COVID-19) from X-ray images. *Medical hypotheses*, 140, 109761.
[5] Ozturk T., Talo M., Yildirim E. A., Baloglu U. B., Yildirim O. and Acharya U. R. (2020). "Automated detection of COVID-19 cases using deep neural networks with X-ray images", *Comput. Biol. Med.*, 121.
[6] Wang, L., Lin, Z. Q., & Wong, A. (2020). Covid-net: A tailored deep convolutional neural network design for detection of covid-19 cases from chest x-ray images. *Scientific Reports*, 10(1): 1-12.
[7] Mayya, A., & Khozama, S. (2020). A Novel Medical Support Deep Learning Fusion Model for the Diagnosis of COVID-19. *In 2020 IEEE International Conference on Advent Trends in Multidisciplinary Research and Innovation (ICATMRI)*, 1-6.
[8] Kedia, P., & Katarya, R. (2021). Covent-19: A Deep Learning model for the detection and analysis of COVID-19 patients. *Applied Soft Computing*, 104, 107184.
[9] Haghanifar, A., Majdabadi, M. M., Choi, Y., Deivalakshmi, S., & Ko, S. (2022). Covid-connect: Detecting covid-19 in frontal chest x-ray images using deep learning. *Multimedia Tools and Applications*, 1-31.
[10] Ye Z., Zhang Y., Wang Y., Huang Z., and Song B., (2020). "Chest CT manifestations of new coronavirus disease 2019 (COVID-19): a pictorial review," *European Radiology*, 30(8):4381-4389.
[11] Bernheim A., Mei X., Huang M., Yang Y., Fayad Z. A., Zhang N. and Diao K., (2020). "Chest CT findings in coronavirus disease-19 (COVID-19): relationship to duration of infection," *radiology*.
[12] Hamdan H. Z., Elgaili Y. O. and Dosogi W. A. A., (2020). "Natural resistance-associated macrophage protein-1 gene polymorphisms and genetic susceptibility to pulmonary tuberculosis in Sudanese patients," *Buletinul Academiei de Ştiinţe a Moldovei. Ştiinţe Medicale*, 69(1):63-72.
[13] Wu J. X., Guo D., Fang Z., Chen L., Huang H. and Li C., (2020). "Chest CT findings in patients with coronavirus disease 2019 and its relationship with clinical features," *Investigative Radiology*, 55(5).
[14] Gillespie M., Flannery P., Schumann J. A., Dincher N., Mills R., and Can A., (2020). "Crazy-paving: a computed tomographic finding of coronavirus disease 2019," *Clinical Practice and Cases in Emergency Medicine*, 4(3).
[15] Shi H., Han X., Jiang N., Cao Y., Alwalid O., Gu J., Fan Y., and Zheng C., (2020). "Radiological findings from 81 patients with COVID-19 pneumonia in Wuhan, China: a descriptive study," *The Lancet infectious diseases*, 20(4):245-434.
[16] K. Li, J. Wu, F. Wu, D. Guo, L. Chen, Z. Fang, and C. Li, "The clinical and chest CT features associated with severe and critical COVID-19 pneumonia," Investigative Radiology, 2020.
[17] Cai Y., Liu J., Yang H., Chen T., Yu Q., Chen J. and Huang D., (2021). "Correlation between early features and prognosis of symptomatic COVID-19 discharged patients in Hunan, China," *Scientific Reports*, 11(1):1-9.
[18] Han R., Huang L., Jiang H., Dong J., Peng H. and Zhang D., (2020). "Early Clinical and CT Manifestations of Coronavirus Disease 2019 (COVID-19) Pneumonia," *American Journal of Roentgenology*, 215(2):338-343.
[19] Rasuli B., "Crazy paving pattern in COVID-19 pneumonia," radio media, 2020. [Online]. Available: https://radiopaedia.org/cases/crazy-paving-pattern-in-covid-19-pneumonia. [Accessed 10 8 2022].
[20] Kurani A., Doshi P., Vakharia A. and Shah M., (2021). "A comprehensive comparative study of artificial neural network (ANN) and support vector machines (SVM) on stock forecasting," *Annals of Data Science*, 1-26.
[21] Alyasseri Z. A. A., Al-Betar M. A., Doush I. A., Awadallah M. A., Abasi A. K., Makhadmeh S. N., and Alomari O. A., "Review on COVID-19 diagnosis models based on machine learning and deep learning approaches," *Expert systems*, 39(3).
[22] Szegedy C., Liu W., Jia Y., Sermanet P., Reed S., Anguelov D., Erhan D., Vanhoucke V. and Rabinovich A., (2015). "Going Deeper with Convolutions," *In Proceedings of The IEEE Conference On Computer Vision and Pattern Recognition, Boston, Massachusetts*.
[23] He K., Zhang X., and R S., (2016). "Deep residual learning for image recognition," *in Proceedings of The IEEE Conference On Computer Vision and Pattern Recognition, Las Vegas, NV, USA*.
[24] COVID-CT dataset. [online], available at: https://github.com/UCSD-AI4H/COVID-CT.